arXiv:cond-mat/0207172v1 [cond-mat.stat-mech] 6 Jul 2002

Dynamical Superfluid-Insulator Transition in a Chain of Weakly Coupled Bose-Einstein Condensates

A. Smerzi[1], A. Trombettoni[1,2], P.G. Kevrekidis[3] and A.R. Bishop[1]

[1] *Theoretical Division and Center for Nonlinear Studies, Los Alamos National Laboratory, Los Alamos, NM 87545, USA*

[2] *Istituto Nazionale di Fisica per la Materia and International School for Advanced Studies, via Beirut 2/4, I-34014, Trieste, Italy*

[3] *Department of Mathematics and Statistics, University of Massachusetts, Amherst, MA 01003-4515, USA*

(February 6, 2008)

We predict a dynammical classical superfluid-insulator transition (CSIT) in a Bose-Einstein condensate (BEC) trapped in an optical and a magnetic potential. In the tight-binding limit, this system realizes an array of weakly-coupled condensates driven by an external harmonic field. For small displacements of the parabolic trap about the equilibrium position, the BEC center of mass oscillates with the relative phases of neighbouring condensates locked at the same (oscillating) value. For large displacements, the BEC remains localized on the side of the harmonic trap. This is caused by a randomization of the relative phases, while the coherence of each individual condensate in the array is preserved. The CSIT is attributed to a discrete modulational instability, occurring when the BEC center of mass velocity is larger than a critical value, proportional to the tunneling rate between adjacent sites.

PACS: 63.20.Pw, 05.45.-a

The recent experimental investigations of the dynamical properties of a Bose-Einstein condensate trapped in optical potentials [1–4], have led to a rapidly growing interest in this topic [5–10]. The spatial and temporal coherence of matter waves emitted at different heights of the gravitational field has been proven in [1], after loading a condensate in a vertical optical trap. Number squeezed (non-classical) states have been realized in [2]. In [3] Bloch oscillations and interband transitions in an accelerating lattice have been observed. In [4], the optical potential was superimposed on a harmonic magnetic trap, realizing a chain of weakly coupled condensates (i.e., a Josephson junction array) driven by an external parabolic field. For small initial displacements, the condensate center of mass oscillated symmetrically with the relative phases among adjacent sites locked togheter.

Here we demonstrate that for large displacements, when the velocity of the center of mass reaches a critical value (proportional to the tunneling rate beteen adjacent sites), the BEC abruptly stops on the side of the harmonic trap (i.e., without reaching its center). We define an order parameter for the system, and show that this dynamical transition from a "superfluid" to an "insulator" regime is associated with a randomization of the relative phases among different wells. As we will discuss below, this transition has a *classical* (mean-field or Gross-Pitaevskii) nature, and it is different (but with some analogies) from the *quantum* superfluid-insulator (Mott) transition caused by the number squeezing of the quantum states in each well [9]. It also differs from the Landau dissipation mechanism, occurring in (quasi-)homogeneous systems when the velocity of the condensate is larger than the sound speed [6]. Rather, the CSIT is driven by a modulational instability (MI) that causes an exponential growth of small perturbations of a carrier wave, as a result of the interplay between dispersion and nonlinearity. The MI is a general feature of discrete as well as continuum nonlinear wave equations. Its demonstrations span a diverse set of disciplines ranging from fluid dynamics [11] (where it is usually referred to as the Benjamin-Feir instability) and nonlinear optics [12] to plasma physics [13]. One of the early contexts in which its significance was appreciated was the linear stability analysis of deep water waves. It was only much later recognized that the conditions for MI would be significantly modified for discrete settings relevant to, for instance, the local denaturation of DNA [14] or coupled arrays of optical waveguides [15]. In the latter case, the relevant model is the discrete nonlinear Scrödinger equation (DNLS), and its MI conditions were discussed in [16]. In this letter we propose an experiment to observe a superfluid-insulator mean-field dynamical transition (as a consequence of the MI), with weakly coupled Bose-Einstein condensates driven by an external harmonic field.

The BEC dynamics is governed by the Gross-Pitaevskii equation (GPE):

$$i\hbar\frac{\partial\Phi}{\partial t} = -\frac{\hbar^2}{2m}\nabla^2\Phi + [V_{ext} + g_0 \mid \Phi \mid^2 - \mu]\Phi \qquad (1)$$

where $g_0 = \frac{4\pi\hbar^2 a}{m}$, a is the s-wave scattering length, m the atomic mass and μ the chemical potential. The condensate wave function $\Phi(\vec{r},t)$ is normalized to the total number of condensate atoms N_T, and we consider a repulsive interatomic interaction $a > 0$. The external potential V_{ext} is given by the sum of the harmonic confining potential $V_M = \frac{m}{2}[\omega_x x^2 + \omega_r^2(y^2+z^2)]$ and the optical potential $V_L = V_0 \cos^2(kx)$. The valleys of the potential are

separated by a "lattice spacing" of $\lambda/2$, with $\lambda = 2\pi/k$. We consider a chemical potential $\mu << V_0$ and the transverse degrees of freedom to be frozen by a tight magnetic confinement, so as to justify the study of the system in an effective one-dimensional geometry.

In the tight-binding approximation $\Phi(\vec{r},t) = \sqrt{N_T}\sum_n \psi_n(t)\phi_n(\vec{r})$, with the wavefunction ψ_j of the condensate in the j-th site of the array, weakly coupled in the barrier region with the wavefunctions $\psi_{j\pm1}$ of the condensates in the neighbour sites. It is then possible to map the GPE onto the DNLS [7]:

$$i\hbar\frac{\partial\psi_n}{\partial t} = -K(\psi_{n-1}+\psi_{n+1}) + (\epsilon_n + U \mid \psi_n \mid^2)\psi_n \quad (2)$$

with $K \simeq -\int d\vec{r}\left[\frac{\hbar^2}{2m}(\vec{\nabla}\phi_n\cdot\vec{\nabla}\phi_{n+1}) + \phi_n V_{ext}\phi_{n+1}\right]$ proportional to the microscopic tunneling rate between adjacent sites, $U = g_0 N_T\int d\vec{r}\phi_n^4$ and $\epsilon_n = \int d\vec{r}[\frac{\hbar^2}{2m}(\vec{\nabla}\phi_n)^2 + V_{ext}\phi_n^2] = \Omega n^2$, with $\Omega = \frac{1}{2}m\omega_x^2\left(\frac{\lambda}{2}\right)^2$. The DNLS Hamiltonian is

$$\mathcal{H} = \sum_n[-K(\psi_n\psi_{n+1}^* + \psi_n^*\psi_{n+1}) + \epsilon_n \mid \psi_n \mid^2 + \frac{U}{2} \mid \psi_n \mid^4] \quad (3)$$

with $i\psi_n^*, \psi_n$ canonically conjugate variables. Both $\mathcal{H}$ and the norm $\sum_n \mid \psi_n \mid^2 = 1$ are integrals of the motion.

Let us consider, first, the case $\epsilon_n = 0$ (which corresponds to neglecting the effect of the harmonic trap). Stationary solutions of Eq. (2) are plane waves $\psi = \psi_0\exp[i(kn-\nu t)]$, of frequency $\nu = -2K\cos(k)+U|\psi_0|^2$. The stability analysis of such states can be carried out by perturbing the carrier wave with small amplitude phonons: $\psi_n = \psi_0 e^{i(kn-\nu t)} + ue^{i(qn-\omega t)} + v^*e^{-i(qn+\omega t)}$. The DNLS excitation spectrum (for $\epsilon_n = 0$) is then given by:

$$\omega_\pm = 2K\sin(k)\sin(q) \pm$$
$$2\sqrt{4K^2\cos^2(k)\sin^4(\frac{q}{2}) + 2KU|\psi_0|^2\cos(k)\sin^2(\frac{q}{2})}. \quad (4)$$

The carrier wave becomes modulationally unstable when the eigenfrequency ω in Eq.(4) becomes imaginary:

$$U|\psi_0|^2 > -2K\cos(k)\sin^2(q/2), \quad (5)$$

namely, when $\cos(k) < 0$. Therefore, if the interatomic interaction is repulsive ($U > 0$), the system suffers an exponential growth of perturbations when $\pi/2 < k < 3\pi/4$. This result will remain valid in the case of non-homogeneous travelling wave-packets driven by external fields, when their width is much larger than the wave length associated with the collective motion. This conclusion can be further understood in the light of the collective coordinate equations of motion developed in [7]. Generally speaking, the mapping of the GPE into the DNLS allows for the study of solitons and localized excitations as well as dynamical instabilities in the framework of the lattice theory [17–19]. We remark, however, that the MI is a general feature of the GPE with a periodic external potential, and not necesserly in the tight binding limit. In the perturbative limit, $\mu >> V_0$, and in absence of external driving fields (i.e., with $V_M = 0$), the MI has been studied in [6,8] (of course, in this limit the MI condition doffers from Eq.(5)).

The effect of the exponential growth of phonon modes of arbitrary momenta in the DNLS leads to an effective dephasing among different sites of the lattice. Indeed the phases of each condensate enter into a "running regime", with an angular velocity different from site to site and proportional to the local (on-site) effective chemical potential. The complete delocalization in momentum space leads to a strong localization in real space, hence to the appearance of localized structures of large amplitude (see Fig. 1). This localization has also been attributed (in the absence of any external potential $\epsilon_n = 0$) to the presence of the so-called Peierls-Nabarro barrier [20], which pins such large amplitude solutions [21], not allowing them to propagate. The excess kinetic energy is partially stored to high-frequency internal "ac" oscillations among adjacent wells (see also [22,23]), and partially converted to wakes of small amplitude extended wave radiation [20,25].

The CSIT can be observed experimentally by condensing, firstly, the atomic gas in both the magnetic and the optical trap, and, then, adiabatically displacing the magnetic field from its initial position. For small displacements, in line with the findings of [4], the system coherently oscillates about the center of the potential. If we rewrite $\psi_j = \sqrt{n_j}e^{i\phi_j}$, this implies that the phase difference between sites is given by $\phi_{j+1}(t) - \phi_j(t) = \Delta\phi(t)$. The center of mass $\xi = \sum_j jn_j$ and the phase difference $\Delta\phi$ will then satisfy

$$\hbar\frac{d}{dt}\xi(t) = 2K\ \sin\Delta\phi(t)$$
$$\hbar\frac{d}{dt}\Delta\phi(t) = -2\ \Omega\ \xi(t). \quad (6)$$

Eqs. (6) have the usual form of the Josephson equations [24] and indicate that the overall array of bosonic Josephson junctions behaves as a *single* Josephson junction, whose critical current is $2K/\hbar$. The collective coherence was experimentally demonstrated in [4] by the interference pattern obtained upon releasing the condensates from the optical and magnetic traps.

To monitor the dynamical transition of interest, we define $< k >= \sum_k k|\tilde{\psi}_k|^2 = \Delta\phi$, with $\tilde{\psi}_k$ the Fourier transform of the condensate wave-function. In the coherent, small amplitude oscillations regime, the quasi-momentum $< k >$ exhibits regular oscillations (see Fig. 2). However, for $< k >\geq \pi/2$, the system becomes modulationally unstable and localization ensues. The critical initial displacement ξ_{cr} can therefore be obtained from Eqs. (6) with $\Delta\phi = \pi/2$. In lattice units:

$$\xi_{cr} = \sqrt{\frac{2K}{\Omega}}. \quad (7)$$

In Fig. 2 we plot $< k >$ vs. time for three initial displacements. When $\xi(t = 0)$ is smaller than ξ_{cr}, the average momentum $< k >$ oscillates in accordance with Eq. (6). Note that for $\xi(t = 80)$ the system approaches very close to the instability line. When the initial displacement is larger than the critical value, $< k >$ abruptly drops as soon as it crosses the critical point. This is accompanied by the sudden arresting of the BEC center of mass (cf. Fig. 1) and by a collective dephasing (cf. Fig. 3). The key experimental signature would be the disappearance of the interference fringes after the expansion of the BEC, while the center of mass of the resulting cloud will be resting on the side of the trap's center.

The values of the parameters in DNLS are $V_0 = 5E_R$ with $\lambda = 795\,nm$ and the recoil energy $E_R = \frac{h^2}{2m\lambda^2}$, $N_T = 50000$, $K = 5.5 \cdot 10^{-2} E_R$ and $\Omega = 1.5 \cdot 10^{-5} E_R$: the critical displacement from Eq. (7) is $\xi_{cr} \approx 84$ sites, in good agreement with our numerical findings (cf. Figs 2 and 3). The loss of coherence is highlighted in Fig. 3, where we plot the temporal evolution of the modulus squared of an effective complex order parameter measuring the overall coherence of the system, defined as:

$$\Psi = \sum_j \psi_j \psi^*_{j+1}. \quad (8)$$

When the collective oscillations are coherent, the value of the order parameter is $|\Psi(t)|^2 = 1$ (see the cases $\xi(t = 0) = 40, 80$ in Fig. 3). On the other hand, a complete dephasing is characterized by $|\Psi(t)|^2 = 0$, and occurs for $\xi(t = 0) \geq \xi_{cr}$, or, equivalently, when $< k > \geq \pi/2$ (cf. Fig. 2). It is worth noting that such randomization takes place between the phases of condensates localized in different wells, even though each one remains internally coherent. This is shown in Fig. 1, where we plot the density for different times below (a,b) and above (c,d) the critical displacement. The numerical solutions of the DNLSE and the GPE are in good agreement. The motion of the center of mass in the supercritical case is reported in Fig. 4, where the numerical solutions of the DNLS and the full one-dimensional GPE (1) are compared. In both cases the system stops at $< x > \simeq 35$ μm (with a slight difference between the DNLS and the GPE predictions), while the center of the harmonic trap is located at $x = 0$ μm. From Eqs. (6) we can calculate the critical current, i.e., the maximum allowed velocity in the coherent transmission of matter waves: by setting $\Delta\phi = \pi/2$ we readily see that the critical velocity of the center of mass, $\dot{\xi}_{max}$ is equal to the critical current per particle $I_c = 2K/\hbar$. In dimensional units:

$$v_c = \frac{K\lambda}{\hbar} \quad (9)$$

which gives $v_c = 0.98$ $\mu m/ms$, in agreement with the DNLS numerical result, and close to the numerical GPE value $v_c = 1.18$ $\mu m/ms$.

From the above findings, we can conclude that the effect of the MI is to dephase the system. In the effective 1D geometry we have considered, such dephasing is strong enough to stop the falling condensate. In higher dimensions, the dephasing can be partial, and will only damp the BEC motion. Yet, its onset will still be given by Eq. (9). The CSIT regards a classical field (the solution of the GPE) and it is qualitatively different from the quantum Mott insulator-superfluid transition in mesoscopic Josephson junction chains, which is driven by the competition between zero-point quantum phase fluctuations and the Josephson coupling energy. Yet, it is possible to draw an analogy. In the former CSIT case, the insulator regime is associated with a vanishing temporal correlation among the phases of each site, each phase still being meaningful in the GPE sense. The quantum transition is also driven by a loss of phase correlations induced by the localization of atoms in each site, which, however, arises from the non-commuting nature of the number-phase observables. Clearly, such quantum fluctuations cannot be captured within the GPE framework. Also, the latter transition is reversible (i.e., long-range phase coherence is restored upon adiabatically increase of the tunnel coupling), while the former is not. It is worth noting that very recent experimental works [26] have illustrated the existence (and reversibility) of the quantum phase transition, rendering the experimental verification of the classical dynamic transition suggested herein, a natural next step for experimental studies. In conclusion, we notice that the MI can be studied in term of one (or several) bifurcation points in an effective stationary Hamiltonian. Such bifurcation points separate regions with different symmetries, and it is common in the literature to study such dynamical transitions in terms of an order parameter [27], borrowing the language and concepts of statistical phase transitions. This mapping, in the specific case of MI, deserves further studies.

The modulational instability (and the consequent superfluid-insulator transition) studied here can also be observed with different experimental setups (e.g., with the condensate at the center of the harmonic trap and with the laser moving across). In fact, similar MI and pinning results have been obtained in the case in which the harmonic trap is displaced at a constant speed exceeding a critical value [28]. These results illustrate the generality and importance of the effects of the MI mechanism in the motion of Bose-Einstein condensates and underscore its potential in inducing localization and dephasing of such coherent structures.

[1] B.P. Anderson and M.A. Kasevich, Science **282**, 1686

(1998).
[2] C. Orzel, A. K. Tuchman, M. L. Fenselau, M. Yasuda, M. A. Kasevich, *Science* **291**, 2386 (2001).
[3] O. Morsch, J.H. Müller, M. Cristiani, D. Ciampini and E. Arimondo, Phys. Rev. Lett. **87**, 140402 (2001)
[4] F.S. Cataliotti, S. Burger, C. Fort, P. Maddaloni, F. Minardi, A. Trombettoni, A. Smerzi and M. Inguscio, Science **293**, 843 (2001).
[5] M.L. Chiofalo and M.P. Tosi, Phys. Lett. A **268**, 406 (2000).
[6] B. Wu and Q. Niu, Phys. Rev. A **64**, 061603(R) (2001).
[7] A. Trombettoni and A. Smerzi, Phys. Rev. Lett. **86**, 2353, (2001).
[8] V.V. Konotop and M. Salerno, cond-mat/0106228.
[9] D. Jaksch et al., Phys. Rev. Lett. **81**, 3108 (1998)
[10] P. Pedri et al., Phys. Rev. Lett. **87**, 220401 (2001)
[11] T.B. Benjamin and J.E. Feir, J. Fluid. Mech. **27**, 417 (1967).
[12] L.A. Ostrovskii, Sov. Phys. JETP **24**, 797 (1969).
[13] T. Taniuti and H. Washimi, Phys. Rev. Lett. **21**, 209 (1968); A. Hasegawa, Phys. Rev. Lett. **24**, 1165 (1970).
[14] M. Peyrard, T. Dauxois, H. Hoyet and C.R. Willis, Physica **68D**, 104 (1993).
[15] R. Morandotti, U. Peschel, J.S. Aitchison, H.S. Eisenberg and Y. Silberberg, Phys. Rev. Lett. **83**, 2726 (1999).
[16] Yu.S. Kivshar and M. Peyrard, Phys. Rev. A **46**, 3198 (1992).
[17] A.C. Scott, "Nonlinear Science: Emergence and Dynamics of Coherent Structures", Oxford Univ. Press, Oxford, 1999
[18] D. Hennig and G.P. Tsironis, Phys. Rep. **307**, 333 (1999).
[19] P.G. Kevrekidis, K.Ø. Rasmussen and A.R. Bishop, Intn. J. Mod. Phys. B **15**, 2833 (2001).
[20] M. Peyrard and M. Kruskal, Physica **14D**, 88 (1984).
[21] T. Dauxois and M. Peyrard, Phys. Rev. Lett. **70**, 3935 (1993).
[22] Yu.S. Kivshar, D.E. Pelinovsky, T. Cretegny and M. Peyrard, Phys. Rev. Lett. **80**, 5032 (1998).
[23] P.G. Kevrekidis and C.K.R.T. Jones, Phys. Rev. E **61**, 3114 (2000).
[24] A. Barone and G. Paterno, *Physics and Applications of the Josephson Effect* (Wiley, New York, 1982).
[25] P.G. Kevrekidis and M.I. Weinstein, Physica **142D**, 113 (2000).
[26] M. Greiner *et al.*, Nature **415**, 39 (2002)
[27] H. Haken, "Synergetics", Springer-Verlag Berlin (1977); G. Venkataraman and V. Balakrisnan, "Sinergetica ed Instabilita' dinamiche", Course IC, Proceedings of the International School of Physics "Enrico Fermi", Varenna, Caglioti, Haken and Lugiato Ed.s, (1988), 175
[28] A. Smerzi, A. Trombettoni, P.G. Kevrekidis and A.R. Bishop (unpublished).

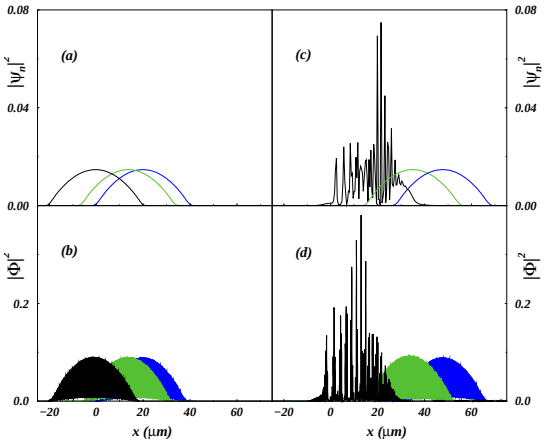

FIG. 1. The density calculated at different times 0, 20, 40 ms (from the right of each figure to the left) as a function of the position, with initial displacements $\xi_(0) = 50, 120$ sites, which are, respectively, below and above the critical value $xi_{cr} \approx 84$ (7). The GPE (b,d), and the DNLS (a,c) wavefunctions normalized to 1 are compared. (a,b) $\xi_(0) = 50$ sites; (c,d) $\xi_(0) = 120$ sites. The external parabolic potential, which drives the oscillations, is centered at $x = 0$.

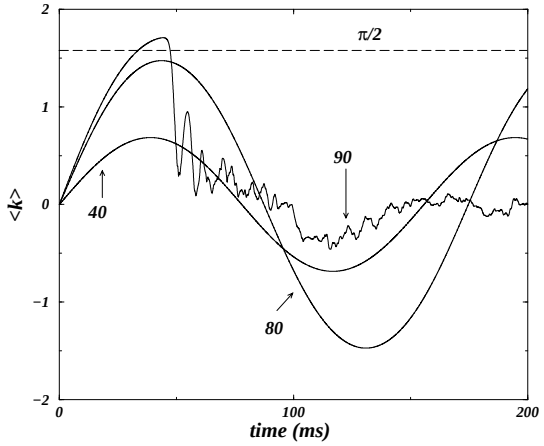

FIG. 2. The quasi-momentum $< k >$ vs. time for three different initial displacements: 40, 80 and 90 sites. When $< k >$ reaches $\pi/2$ (i.e., for an initial displacement greater than $\xi_{cr} \approx 84$ calculated with Eq.(7) the system becomes modulationally unstable.

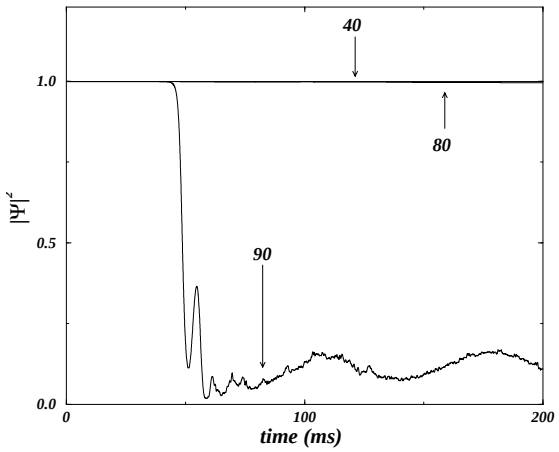

FIG. 3. The modulus square of the order parameter Ψ defined in Eq. (8) as a function of time, for three different initial displacements (40, 80 and 90 sites) and with the same parameters as in Fig. 2. When the quasi-momentum $< k >$ reaches $\pi/2$ (i.e., for an initial displacement greater than ξ_{cr}), the order parameter drops to ~ 0; cf. Fig. 2.

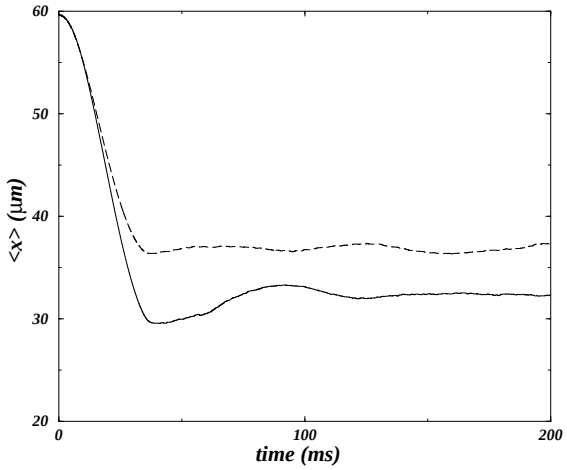

FIG. 4. The center of mass vs. time for a supercritical initial displacement of 150 sites. Solid line: Gross-Pitaevskii equation; dashed line: discrete nonlinear Schrödinger equation. The (displaced) center of the trap is at $x = 0$ μm.